Tumor Necrosis Factor-α and *Porphyromonas gingivalis* Lipopolysaccharides Decrease Periostin in Human Periodontal Ligament Fibroblasts

Miguel Padial-Molina,* Sarah L. Volk,* Juan C. Rodriguez,* Julie T. Marchesan,* Pablo Galindo-Moreno,† and Hector F. Rios*

Background: Periostin is a matricellular protein essential for tissue integrity and maturation and is believed to have a key function as a modulator of periodontal ligament (PDL) homeostasis. The aim of this study is to evaluate whether periodontal disease-associated pathogen-related virulence factors (endotoxins/lipopolysaccharides [LPS]) and proinflammatory cytokines alter the expression of periostin in PDL cells.

Methods: Human PDL cultures were exposed to inflammatory mediators (tumor necrosis factor-α [TNF-α]), bacterial virulence factors (*Porphyromonas gingivalis* LPS) or a combination in a biomechanically challenged environment. Culture conditions were applied for 24 hours, 4 days, and 7 days. Periostin and TGF-β inducible gene clone H3 (βIGH3) mRNA expression from cell lysates were analyzed. Periostin and βIGH3 proteins were also detected and semiquantified in both cell lysates and cell culture supernatants by Western blot. In addition, periostin localization by immunofluorescence was performed. Analysis of variance and Fisher tests were used to define the statistical differences among groups ($P<0.05$).

Results: In a mechanically challenged environment, periostin protein was more efficiently incorporated into the matrix compared to the non-loaded controls (higher levels of periostin in the supernatant in the non-loaded group). Interestingly, chronic exposure to proinflammatory cytokines and/or microbial virulence factors significantly decreased periostin protein levels in the loaded cultures. There was greater variability on βIGH3 levels, and no particular pattern was clearly evident.

Conclusions: Inflammatory mediators (TNF-α) and bacterial virulence factors (*P. gingivalis* LPS) decrease periostin expression in human PDL fibroblasts. These results support a potential mechanism by which periostin alterations could act as a contributing factor during periodontal disease progression. *J Periodontol 2013;84:694-703.*

KEY WORDS

βIG-H3 protein; lipopolysaccharides; periodontal diseases; periodontal ligament; periostin protein, human; tumor necrosis factor-alpha.

* Department of Periodontics and Oral Medicine, School of Dentistry, University of Michigan, Ann Arbor, MI.
† Department of Oral Surgery and Implant Dentistry, School of Dentistry, University of Granada, Granada, Spain.

doi: 10.1902/jop.2012.120078

Periostin (gene POSTN) is an 835 amino acid in humans, 90 kDa secreted adhesion molecule of the fasciclin family that contains four tandem Fas domains homologous to Fasciclin-I.[1] Periostin is highly expressed in the periodontal ligament (PDL) and other fibrous connective tissues, such as periosteum, perichondrium, tendons, cornea, and heart valves.[2] Periostin knock-out (KO) mice have been reported as normal at birth, but later develop dwarfism and a compromised periodontium.[3] In the periosteum and PDLs, periostin has been demonstrated as essential for tissue integrity, tooth development, the eruption process,[3-5] recruitment and attachment of osteoblast precursors,[6] and modulator of osteoblast differentiation.[7] Moreover, periostin can be described as the protein that reflects periodontal functionality because of its higher expression in response to occlusal loading or orthodontic movement.[7]

Periostin is highly homologous to transforming growth factor-β (TGF-β) inducible gene clone H3 (βIGH3) (68 kDa). Both genes are induced by TGF-β1, known to regulate matrix production under biomechanical stimulation,[6] and colocalize in the PDL.[8] Both fasciclins modulate the matrix–cell interactions, relevant to connective tissue repair and remodeling, as well as fibroblast attachment and spreading.[9,10]

In humans, the main reason for loss of periodontal tissue integrity is periodontal disease caused by bacteria acting in a susceptible host.[11] Many inflammatory mediators and cytokines have been reported to act in this scenario, leading to alveolar bone loss. In addition, TGF-β signaling is involved in fibroblast–epithelial cell interaction in periodontitis associated with aggressive matrix destruction.[12]

In brief, periostin is key in maintaining periodontal stability in relation to mechanical function. Periodontal diseases imply both bacterial pathogenesis and host response mediated by cytokines. Therefore, we hypothesize that inflammatory mediators and bacterial virulence factors act as a complex regulatory pathway that modifies the periostin expression under mechanical stimulation, which constitutes a cofactor for periodontal destruction and disease progression. Hence, the aim of this study is to analyze the influence of inflammatory and infectious processes on periostin expression.

MATERIALS AND METHODS

Cell Populations

Primary human PDL (hPDL) fibroblasts obtained from maxillary premolar teeth of two adult healthy patients (one male and one female, aged 29 and 35 years, respectively) are used in this study and are identical to those cells used in a recent study regarding cell proliferation and differentiation.[13] Both cell populations were generously donated by the group of Dr. William V. Giannobile (senior author of that study), University of Michigan, Ann Arbor, Michigan. Cells were maintained in Dulbecco's modified Eagle's medium‡ supplemented with 10% fetal bovine serum,§ antibiotics (100 U/mL penicillin and 100 µg/mL streptomycin), antifungal (1:1,000 amphotericin B), and 2 mM glutamine, at 37°C in a humidified atmosphere of 95% air–5% CO_2. Cells were removed from the growth surface with a trypsin solution (0.25% trypsin, 0.1% glucose, and citrate–saline buffer [pH 7.8])‖ and subsequently used for experiments. Von Kossa staining was done and compared to two other hPDL cell populations to confirm the fibroblastic phenotype. The populations with less mineralization potential after 1 week of supplementation with L-ascorbic acid (1:1,000 dilution of a 50 mg/mL stock solution¶) and sodium phosphate (1:100 dilution of a 300 mmol stock#) were selected. Cells were used between passages 4 and 7 for experiments. Three separate experiments were done for all primary hPDL populations. The analysis of each sample was done in triplicate.

Porphyromonas gingivalis LPS Purification

P. gingivalis (*Pg* 2561) (American Type Culture Collection [ATCC] 33277) was grown in prereduced *Brucella* broth enriched with 5 mg/mL hemin and 1 µg/mL menadione in an atmosphere of 5% hydrogen, 10% carbon dioxide, and 85% nitrogen at 37°C. Lipopolysaccharides (LPS) were extracted from bacteria by the method of Darveau and Hancock.[14] LPS was then subjected to sodium dodecyl sulfate-polyacrylamide gel electrophoresis (SDS-PAGE) and stained by silver and blue** stainings. The same tests were performed with other strains to compare purity of the LPS derivative, including commercial LPS (*Escherichia coli* [*E. coli*] 055:B5††) and derivates from *E. coli* DSM 1103, *Pg* W83, and *Fusobacterium nucleatum* (*F. nucleatum*) VPI 4355.‡‡

After purification, LPS preparation was lyophilized, resuspended in Connaught Medical Research Laboratories media, and stored at –20°C for additional in vitro use.

Cell Culture Conditions

Cells were plated in flexible-bottom six-well plates§§ at 250,000 cells per well. At 24 hours after seeding,

‡ DMEM, Invitrogen, Grand Island, NY.
§ Invitrogen.
‖ Invitrogen.
¶ Sigma-Aldrich, St. Louis, MO.
# Sigma-Aldrich.
** Coomassie brilliant blue, Invitrogen.
†† L2880, Sigma-Aldrich.
‡‡ *E. coli* DSM 1103 = 25922 ATCC; *P.gingivalis* W83 = BAA-308 ATCC; *F. nucleatum* VPI 4355 = 25586 ATCC, American Type Culture Collection, Manassas, VA.
§§ BioFlex Culture Plates coated with Collagen I, Flexcell International, Hillsborough, NC.

wells were assigned to four different groups: 1) control; 2) *Pg* LPS; 3) TNF-α; and 4) TNF-α + *Pg* LPS. The media were changed to fresh media supplemented with 10 ng/mL TNF-α,‖‖ 200 ng/mL *Pg* LPS, or a combination. All supplemented media included L-ascorbic acid (1:1,000 dilution of a 50 mg/mL stock solution¶¶). Cultures were subjected to biomechanical stimulation## (loaded with 14% stretching at six cycles per minute) during the entire experiment (24 hours, 4 days, and 7 days). Media were changed every 24 hours.

To compare with non-loaded culture conditions, a similar set of cultures was done in regular six-well plates and supplemented in the same way. In this case, 10 ng/mL TGF-β1*** was also added to compare its stimulatory effect versus the stimulatory effect of mechanical stimulation. In each set of cultures (loaded in flexible-bottom wells and non-loaded in regular plates) one unstimulated condition was also analyzed. These unstimulated conditions included culture in regular plates without TGF-β1 and culture in flexible-bottom plates without mechanical stimulation.

mRNA Assay and Reverse Transcriptase-Quantitative Polymerase Chain Reaction

At the times mentioned above, supernatant was removed, and cells were washed twice with phosphate-buffered saline (PBS) and collected by scraping in lysis buffer. RNA was then isolated.†††

Reverse transcriptase-polymerase chain reaction (RT-PCR) was performed using a thermal cycler‡‡‡ immediately after RNA isolation. The RT mix§§§ was made for a final volume of 50 µL complementary deoxyribonucleic acid (cDNA) (2 µg RNA and oligo-dT primer). The probes used in the quantitative PCR‖‖‖‖ were POSTN (Hs01566748_m1), βIGH3 (Hs00932734_m1), and GAPDH (Hs99999905_m1). Each plate contained triplicates of the cDNA templates. The $2^{\Delta\Delta Ct}$ method was used to calculate gene expression levels relative to GAPDH.

Western Blot of Lysates and Supernatant

In a different set of cultures, at the times mentioned above, 1 mL supernatant was collected from each group, concentrated using 30,000 membrane centrifugal filters,¶¶¶ diluted in 400 µL PBS, and stored at –80°C until analysis. Excess supernatant was removed, and cells were washed twice with PBS and collected by scraping. Cell–PBS mixture was spun at 3,000 rpm for 10 minutes at 4°C to pellet the cells. Cell pellets were resuspended in lysis buffer (0.1 M Tris [pH 6.8], 2% SDS, 1% β-mercaptoethanol, and 1:100 protease inhibitor cocktail), vortexed for 5 minutes, and incubated on ice for 30 minutes. The lysates were centrifuged again (12,000 rpm for 10 minutes at 4°C), and protein supernatants were collected.

For both cell lysates and cell culture supernatant, total protein concentration was quantified using the microassay Bradford method### and read using a plate reader**** at a wavelength of 595 nm. Total protein (25 µg) from each solution was run on 10% SDS-PAGE gels (100 V, 2 hours), electroblotted onto polyvinylidene difluoride membranes (90 V, 90 min), blocked (5% milk in Tris-buffered saline with 0.1% of Tween 20 [pH 7.4], 1 hour), and immunoprobed for periostin (0.25 µg/mL in 5% milk, rabbit polyclonal to periostin†††† overnight; 1:4,000 goat antirabbit immunoglobin [IgG]–horseradish peroxidase [HRP],‡‡‡‡ 1 hour). Membranes were stripped (25 mM glycine and 1% SDS [pH 2.0], for 2 hours), blocked again, and immunoprobed for βIGH3 (0.15 µg/mL in 5% milk, biotinylated anti-human βIGH3§§§§ overnight; 1:3,000 donkey anti-goat IgG–HRP,‖‖‖‖‖ 1 hour), and stripped, blocked, and probed one more time for GAPDH (0.167 µg/mL, in 5% milk, antihuman/mouse/rat GAPDH¶¶¶¶ overnight; 1:4,000 donkey antigoat IgG–HRP,#### 1 hour). Immunopositive bands were detected by enhanced chemiluminescence***** and autoradiography.

Immunolocalization of Periostin in Cell Cultures

After 7 days of exposure to the different culture conditions in another set of cultures, actin, periostin, and 4′,6-diamidino-2-phenylindole (DAPI) staining was performed. Briefly, the culture medium was removed, the cells were washed twice with PBS, and fixation was performed in 4% paraformaldehyde for 10 minutes. Cells were then permeabilized by applying 0.25% non-ionic surfactant††††† for 10 minutes. Filamentous actin (F-actin) distribution was revealed with green fluorescent dye‡‡‡‡‡ (1:40 dilution) for 20 minutes. Immunofluorescence staining for periostin was performed by using an affinity-purified rabbit polyclonal antibody§§§§§ (1:400 dilution) overnight. Immunologic reaction was visualized by using a sheep polyclonal secondary antibody to rabbit

‖‖ Abcam, Cambridge, MA.
¶¶ Sigma-Aldrich.
Flexcell FX-5000 Tension System, Flexcell International.
*** Recombinant human TGF-β1, Invitrogen.
††† Trizol Plus RNA Purification Kit, Invitrogen.
‡‡‡ PTC-200 Peltier Thermal Cycler, MJ Research, GMI, Ramsey, MN.
§§§ Taqman Reverse Transcription Reagents Kit, Applied Biosystems, Invitrogen.
‖‖‖‖ 7500 Real-Time PCR System, Applied Biosystems.
¶¶¶ Millipore, Billerica, MA.
Bio-Rad, Hercules, CA.
**** Multiskan Ascent, Thermo Labsystems, Thermo Fisher Scientific, Waltham, MA.
†††† ab14041, Abcam.
‡‡‡‡ Santa Cruz Biotechnology, Santa Cruz, CA.
§§§§ R & D Systems, Minneapolis, MN.
‖‖‖‖‖ Santa Cruz Biotechnology.
¶¶¶¶ R & D Systems.
Santa Cruz Biotechnology.
***** Thermo Fisher Scientific.
††††† Triton X-100, Acros Organics, Geel, Belgium.
‡‡‡‡‡ Alexa Fluor-488 phalloidin, Invitrogen.
§§§§§ ab14041, Abcam.

conjugated with red fluorescent dye[|||||||] (1:200 dilution) for 1 hour. Slides were then treated with an antifade agent containing DAPI[¶¶¶¶¶] (stains for DNA) and covered with glass coverslips. All stained slides were imaged using a confocal microscope[#####] using the same settings.

Statistical Analyses

Western Blot signal was semiquantified using imaging software.[******] Immunopositive bands were normalized to GAPDH and by assigning a relative value of 1 to the control group at every time point. mRNA fold changes were calculated relative to each control group per time point.

Analysis of variance (ANOVA) and Fisher tests were used to define the statistical differences among groups ($P < 0.05$). Tests were run independently at every time point. Data are shown as mean ± SE.

RESULTS

Pg *LPS Characterization*

Pg cultivation was confirmed by BANA test for positiveness.[15] After the LPS extraction from bacteria by the method of Darveau and Hancock,[14] silver staining confirmed its presence in the SDS-PAGE gel. Furthermore, compared to commercial LPS derived from *E. coli* 055:B5 and those derived from *E. coli* DSM 1103, *Pg* W83, and *F. nucleatum* VPI 4355, the blue staining confirmed no gross amounts of protein contamination of the LPS preparation from *Pg* 2561 (ATCC 33277) (data not shown).

mRNA Assay

Under non-loaded conditions, periostin mRNA expression showed a high variability among the groups with an unclear pattern (Fig. 1A). No statistically significant differences were found ($P > 0.05$, ANOVA).

Interestingly, under biomechanical stimulation, an acute increase in mRNA periostin levels was observed at 24 hours (1 ± 0.0, 1.11 ± 0.04, 1.63 ± 0.08, 1.38 ± 0.10). The increase was significant for TNF-α and TNF-α + *Pg* LPS compared to control ($P < 0.003$ and $P < 0.016$, respectively, Fisher test) and compared to *Pg* LPS ($P < 0.005$ and $P < 0.047$, respectively, Fisher test). In contrast, chronic exposure to inflammatory mediators and bacterial virulence factors, separately or combined, led to a reduction in mRNA periostin expression levels at 4 days (1 ± 0.0, 0.87 ± 0.06, 0.61 ± 0.05, 0.59 ± 0.25) and significantly at 7 days (1 ± 0.0, 0.78 ± 0.05, 0.54 ± 0.12 [$P < 0.015$, Fisher test], 0.57 ± 0.09 [$P < 0.018$, Fisher test]) (control, *Pg* LPS, TNF-α, and TNF-α + *Pg* LPS, respectively) (Fig. 1B).

βIGH3 mRNA expression followed a very similar pattern, under both non-loaded (Fig. 1C) and loaded (Fig. 1D) conditions. However, no significant differences were found at any treatment or any time ($P > 0.05$, ANOVA).

Protein Analyses

After 7 days under non-loaded conditions, TGF-β1 clearly increased periostin protein expression compared to the unstimulated situation (Fig. 2A, U versus C). Thus, treatment with TGF-β1 was established as the non-loaded control. In a similar way, mechanical stimulation clearly increased periostin protein expression compared to the unstimulated situation (Fig. 2B, U versus C). Thus, mechanical stimulation was established as loaded control. Detection of periostin in supernatant from cultures mechanically stimulated required longer exposure times for the same amount of total protein (25 µg). Thus, a higher proportion of total protein remained incorporated within the cell layer.

Under non-loaded conditions, periostin protein detected within the cell lysate (Fig. 3A) compared to control was significantly lower at 4 days (1 ± 0.0, 0.70 ± 0.13 [$P < 0.008$], 0.25 ± 0.05 [$P < 0.001$], 0.25 ± 0.10 [$P < 0.001$]) and 7 days (1 ± 0.0, 1.12 ± 0.08, 0.37 ± 0.27 [$P < 0.001$], 0.51 ± 0.32 [$P < 0.001$]) (control, *Pg* LPS, TNF-α, TNF-α + *Pg* LPS, respectively). However, no significant differences were found in the detection of periostin protein in the supernatant except for an initial increase at 24 hours (1 ± 0.0, 1.08 ± 0.10, 2.11 ± 0.78, 2.83 ± 0.83 [$P < 0.035$]) (control, *Pg* LPS, TNF-α, TNF-α + *Pg* LPS, respectively) (Fig. 3B). βIGH3 showed a similar pattern for all different groups and time points (Fig. 4A): 24 hours: 1 ± 0.0, 2.06 ± 0.41 [$P < 0.037$], 1.59 ± 0.26, 1.69 ± 0.46; 4 days: 1 ± 0.0, 0.99 ± 0.07, 0.62 ± 0.04 [$P < 0.001$], 0.64 ± 0.12 [$P < 0.002$]; 7 days: 1 ± 0.0, 0.75 ± 0.05 [$P < 0.022$], 0.41 ± 0.1 [$P < 0.001$], 0.63 ± 0.09 [$P < 0.001$] (control, *Pg* LPS, TNF-α, TNF-α + *Pg* LPS, respectively) (Fig. 5A). Detection of βIGH3 in the supernatant was significantly reduced at both 4 days (1 ± 0.0, 0.89 ± 0.10, 0.52 ± 0.15 [$P < 0.026$], 0.61 ± 0.22) and 7 days (1 ± 0.0, 1.14 ± 0.09, 0.48 ± 0.15 [$P < 0.003$], 0.57 ± 0.12 [$P < 0.011$]) (control, *Pg* LPS, TNF-α, TNF-α + *Pg* LPS, respectively).

In a similar way, in a mechanically challenged environment, exposure to proinflammatory cytokines (TNF-α) and/or microbial virulence factors (*Pg* LPS) initially increased periostin levels. However, chronic exposure led to decreased periostin protein levels within the cell lysate after 4 days (1 ± 0.0, 1.14 ± 0.02 [$P < 0.014$], 0.81 ± 0.05 [$P < 0.001$], 0.74 ± 0.04 [$P < 0.001$]) and 7 days (1 ± 0.0, 0.91 ± 0.07, 0.55 ± 0.02 [$P < 0.001$], 0.53 ± 0.05 [$P < 0.001$])

[|||||||] ab6793-1 conjugated with Texas Red, Abcam.
[¶¶¶¶¶] ProLong Gold antifade reagent with DAPI, Invitrogen.
[#####] Fluoview 500 confocal microscope, Olympus America, Center Valley, PA.
[******] NIH ImageJ software, National Institutes of Health, Bethesda, MD.

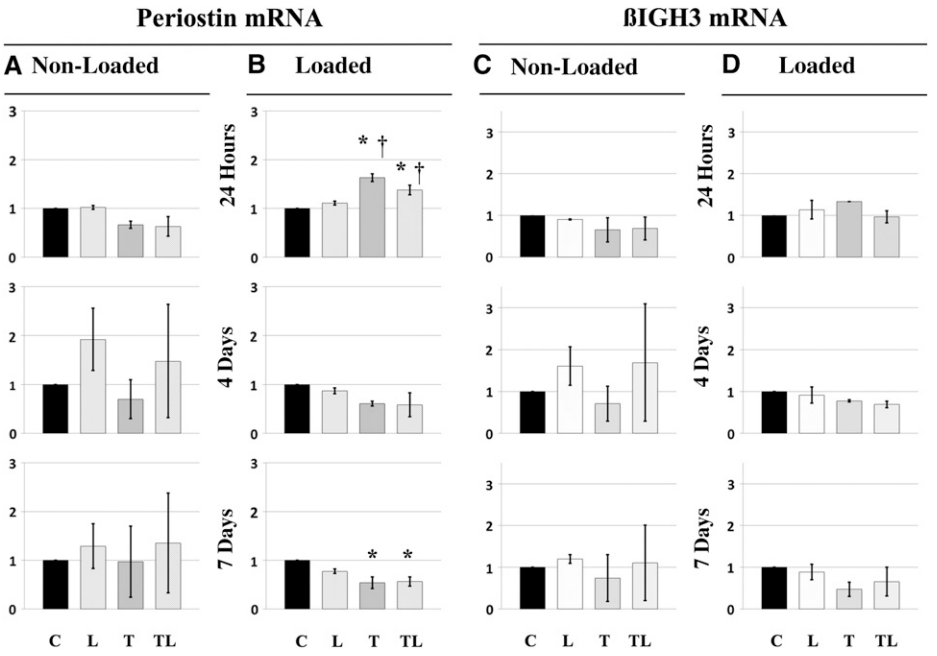

Figure 1.
*Periostin mRNA fold changes relative to control per time point in non-loaded **(A)** and loaded **(B)** conditions at different times. βIGH3 mRNA fold changes relative to control per time point in non-loaded **(C)** and loaded **(D)** conditions at different times. Error bars indicate standard error. Statistically significant differences are indicated (P <0.05): *compared to control conditions; †compared to Pg LPS. C = control; L = Pg LPS; T = TNF-α; TL = TNF-α + Pg LPS.*

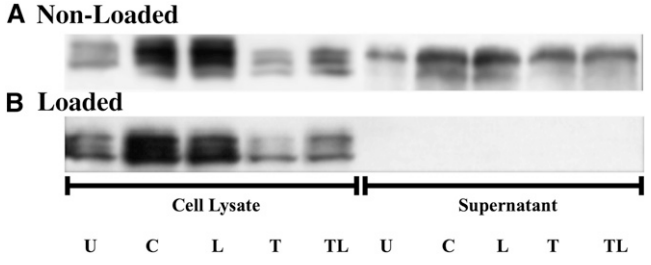

Figure 2.
*Periostin protein detection in cell lysate and supernatant in non-loaded **(A)** and loaded **(B)** conditions at 7 days time point. The same amount of total protein (25 μg) and exposure time (2 minutes) were used for each Western blot. Note that a higher proportion of the total protein remained incorporated within the cell lysate. C = control; L = Pg LPS; T = TNF-α; TL = TNF-α + Pg LPS; U = unstimulated.*

(control, *Pg* LPS, TNF-α, TNF-α + *Pg* LPS, respectively) of exposure (Figs. 3A and 5B). Interestingly, the proportion of periostin protein detectable in the supernatant in relation to the cell lysate was lower than in non-loaded conditions, as mentioned previously (Fig. 2). Furthermore, there were some differences among different treatment groups not found in non-loaded cultures. In this case, periostin in the supernatant was reduced by the effect of TNF-α, *Pg* LPS, or the combination, at 24 hours (1 ± 0.0, 0.55 ± 0.08, 0.25 ± 0.06 [P <0.005], 0.74 ± 0.32), 4 days (1 ± 0.0, 0.48 ± 0.14 [P <0.026], 0.56 ± 0.16, 0.62 ± 0.21), and 7 days (1 ± 0.0, 0.52 ± 0.17 [P<0.032], 0.43 ± 0.09 [P <0.013], 0.53 ± 0.22 [P <0.038]) (control, *Pg* LPS, TNF-α, TNF-α + *Pg* LPS, respectively) (Fig. 3B).

Although alterations were also noticed for βIGH3 under biomechanical stimulation, there was greater variability of the results over time (Fig. 4). βIGH3 seemed to be downregulated by proinflammatory cytokines and bacterial virulence factors at 4 days (1 ± 0.0, 1.41 ± 0.09 [P <0.001], 0.45 ± 0.05 [P<001], 0.44 ± 0.06 [P<0.001]; control, *Pg* LPS, TNF-α, TNF-α + *Pg* LPS, respectively), but a greater variability with no clear pattern could be detected at 7 days (Figs. 4A and 5B). Detection of βIGH3 in the cell culture supernatant showed no significant differences among treatments for any time point (Fig. 4B).

Matrix Maturation and Periostin Localization

Cell culture morphology and organization were, in general, unaffected by the different supplements in the media as demonstrated by F-actin immunolocalization (Fig. 6A). Cells in all cultures looked well organized and oriented and showed typical histomorphologic characteristics of a normal mature fibroblast cell culture, as depicted by simultaneous staining of intracellular F-actin (in green) and DNA structures (DAPI, in blue). However, immunofluorescence staining for periostin (in red) clearly confirmed that chronic exposure (7 days) to proinflammatory cytokines (TNF-α) and/or microbial virulence factors (*Pg* LPS) decreased periostin incorporation into the matrix. Both TNF-α and TNF-α + *Pg* LPS were able to reduce periostin immunodetection because less fiber-like structure was visualized compared to the control group.

DISCUSSION

Today, there is no known cure for periodontitis. It can only be controlled and should be reevaluated at regular intervals. This is particularly important because periodontal diseases collectively afflict >80% of adults worldwide, and ≈13% display severe conditions concomitant with early tooth loss.[16] In general,

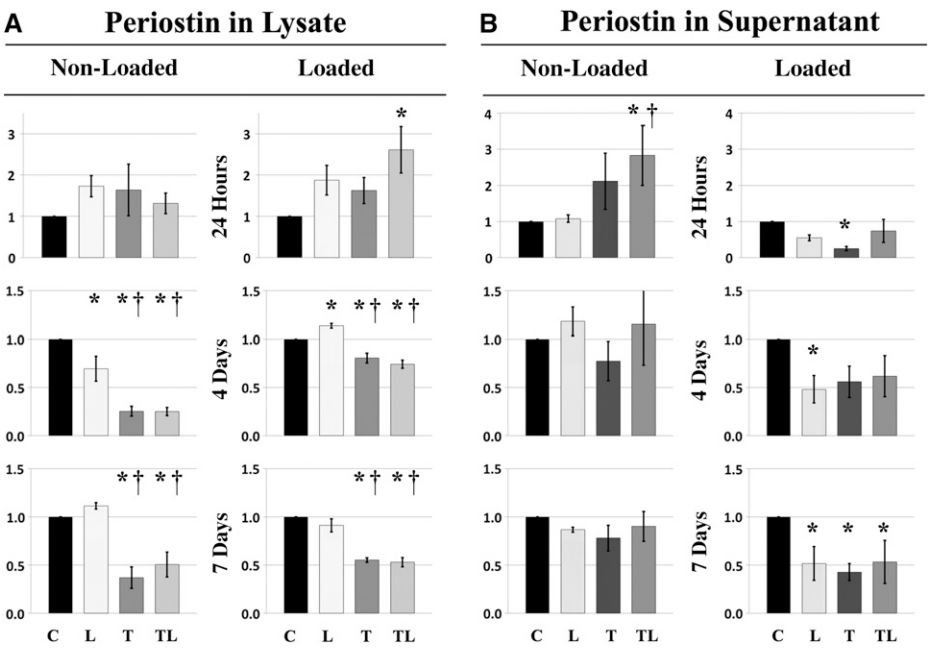

Figure 3.
Periostin protein fold changes relative to control per time point in cell lysate ***(A)*** *and supernatant* ***(B)*** *in non-loaded and loaded conditions at 24 hours, 4 days, and 7 days. Statistically significant differences are indicated (P <0.05):* *******compared to control conditions; †compared to Pg LPS. C = control; L = Pg LPS; T = TNF-α; TL = TNF-α + Pg LPS.*

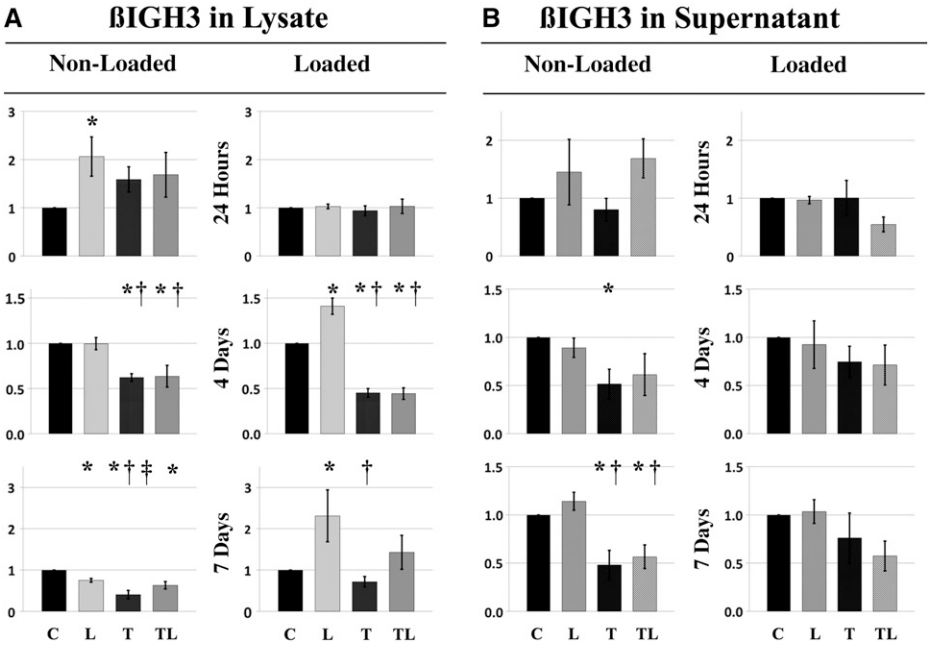

Figure 4.
βIGH3 protein fold changes relative to control per time point in cell lysate ***(A)*** *and supernatant* ***(B)*** *in non-loaded and loaded conditions at 24 hours, 4 days, and 7 days. Statistically significant differences are indicated (P <0.05):* *******compared to control conditions; †compared to Pg LPS; ‡compared to TNF-α + Pg LPS. C = control; L = Pg LPS; T = TNF-α; TL = TNF-α + Pg LPS.*

the detrimental changes that the tooth-supporting tissues undergo during disease are primarily the result of specific microbial challenges[17] in a susceptible host.[11] During health, the structure and properties of the periodontal tissues are intimately related by crucial cell–matrix interactions.[18] The proper regulation of these interactions in a mechanically dynamic environment determines the adaptive dental–alveolar responses.[19,20] The proteins modulating these interactions are collectively known as matricellular molecules. However, the mechanisms by which the modulation of these cell–matrix synergistic events are undermined and compromised during periodontal disease and how they may enhance the tissue healing response are not clearly understood. Periostin, a matricellular molecule highly expressed by PDL fibroblasts, is implicated in periodontal homeostasis and may play a role in periodontal disease.

Periostin is abundantly expressed in collagen-rich fibrous connective tissues that are subjected to mechanical stresses, including endocardial cushions, cardiac valves, tendons, perichondrium, cornea, periosteum, and the PDL.[3,4,6,21-25] Periostin localization in these tissues suggests potential roles in their maintenance and remodeling. Expression of periostin is significantly increased in response to mechanically regulated bone morphogenetic protein (BMP) and TGF-β growth factor (Fig. 2) signaling in mesenchymal cells undergoing differentiation.[6] Periostin directly interacts with type I collagen[22,26] through its EMI domain and with tenascin-C[27] and BMP-1[28] through its Fas-I domains.

Of the known proteins expressed in the PDL, periostin

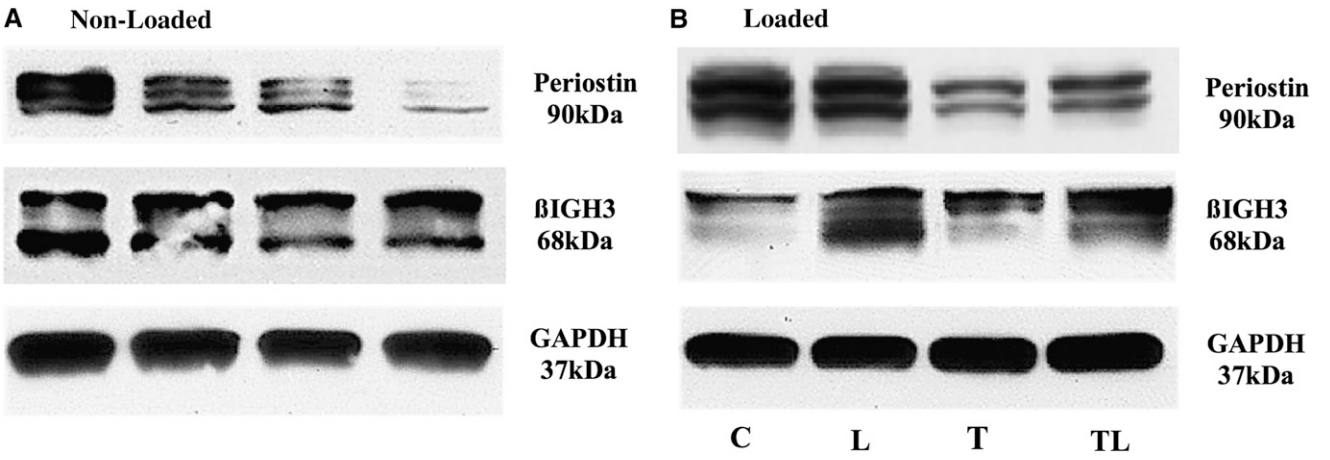

Figure 5.
*Western blot images (25 μg total protein) representing detection of periostin, βIGH3, and GAPDH from cell lysates of the different conditions after 7 days in non-loaded **(A)** and loaded **(B)** situations. C = control; L = Pg LPS; T = TNF-α; TL = TNF-α + Pg LPS.*

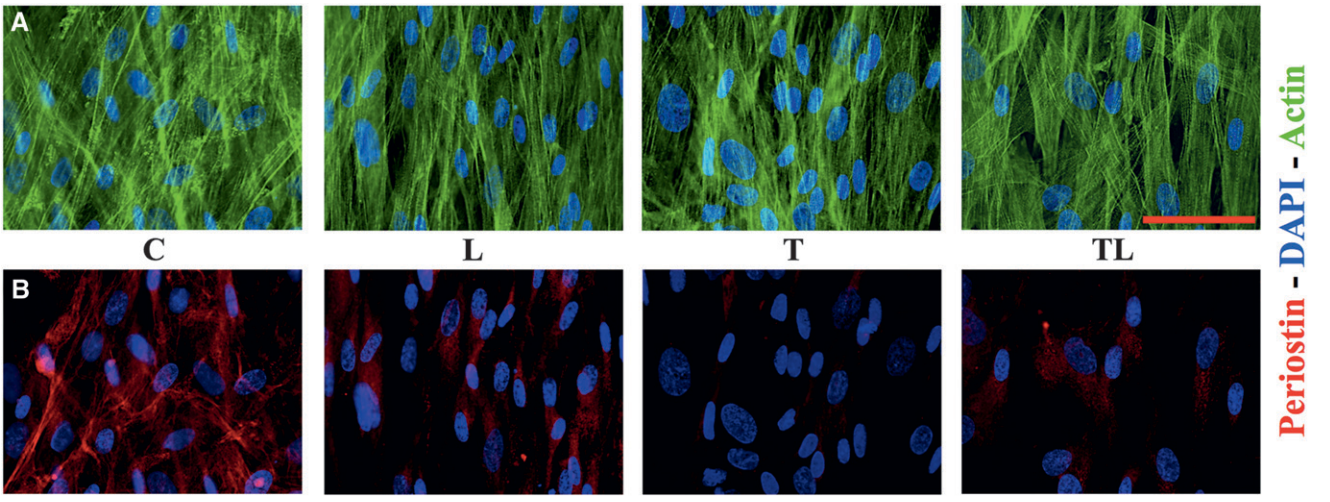

Figure 6.
*Immunofluorescence staining at 7 days. **A)** General morphology observation of the cell layer stain with F-actin (green) and DAPI (blue). **B)** Immunofluorescence detection of periostin (red) and DAPI (blue). Note that periostin detection in the extracellular space forming fibers (in red) is more evident in the control group but reduced in the others. Scale bar = 50 μm. C = control; L = Pg LPS; T = TNF-α; TL = TNF-α + Pg LPS.*

has been the one that shows greater specificity.[29] Furthermore, immunoelectron microscopic observation of the mature PDL verified the localization of periostin between the cytoplasmic processes of periodontal fibroblasts and cementoblasts and the adjacent collagen fibrils.[26,30] For this reason, periostin is commonly used as a marker for the functional and structurally stable PDL.[31]

Periostin is essential in the functional and structural integrity of the periodontium.[3,5,32] Periostin-deficient and KO animals clearly showed severe deterioration of the tooth-supporting structures. Its absence results in a traumatic stimulus to the periodontium.[3,5] Moreover, failure of proper collagen fiber turnover in those animals suggested that periostin may function in the remodeling of the collagen matrix in the shear zone of PDLs.[26]

Defects in the extracellular matrix (ECM) can have major implications in tissue function over time by compromising the structural and functional integrity of the connective tissues. The role of periostin in those processes has been confirmed by morphometric studies that demonstrate reduced diameter of collagen fibrils in periostin KO compared to wild-type mice, which exhibited statistically lower skin tissue strength.[22] Such situations, extrapolated to the

periodontium, may determine the competency of the periodontal tissue to cope with the biomechanical requirements derived from the physiologic tooth-supporting apparatus function. In our study, although normal cellular morphologic appearance was detected (Fig. 6A), reduction in periostin levels (Fig. 6B) might be able to reduce the ability of the ECM–cell complex to support normal mechanical function.[22] Moreover, although no physiologic levels of periostin in the PDL have been reported, it can be assumed that a normal threshold exists and modulates the biomechanical competency of the periodontal ECM.[5]

The periodontium normally adapts to increases in mechanical loading by producing more bone and soft tissue and reorganizing the tissue to accommodate the increased loads. However, in the periostin KO, these adaptation responses are substantially attenuated, indicating that periostin is crucial to the transduction of the mechanical signals. In periostin-deficient animals, the mechanical stimulus leads to severe alveolar bone loss, severe clinical attachment loss, and significant widening of the PDL space, which can be classified as a secondary trauma.[5] In the present study, mechanical stimulation is done under a 14% strain and six cycles per minute regimen. Previous studies[5,33-35] have revealed a time-dependent increase in periostin by using that particular regimen. Furthermore, after cessation of the stretching regimen, periostin mRNA levels rapidly decreased to levels of expression similar to those found in the control group, remaining stable over time. Other strain conditions, either higher (20%) or lower (1%), did not show any significant changes.[5] Stretching regimens from 1% to 20% correspond to ≈0 to 15 N, with 1% representing hypofunctional stimulation, 14% representing normal occlusal stimulation, and 20% representing over-physiologic stimulation.[5,33-35] In vivo, the PDL is exposed to continuous non-stop mechanical stimulation when biting/chewing, swallowing, tongue movements, other muscles movements, etc. Several experimental models for mechanical stress have been developed for in vitro cell culture systems.[5,33-36] However, it has not been possible, until now, to predict the exact force that acts in vivo on the periodontium on the single-cell level or the actual force for an individual tooth.[37] Based on the literature,[5,33-36] the force magnitude and timeframe set in the present in vitro study simulate the in vivo continuous (or "chronic") mechanical challenge that the teeth support when developing periodontal diseases.

In addition, periostin interacts with $\alpha_v\beta_3$ receptors and activates AKT/protein kinase B cell survival pathways.[38,39] Furthermore, periostin increases cell migration, recruitment, and attachment into the healing area in different tissues, including osteoblast precursors,[6] cardiac tissue,[40,41] and skin.[42] It is presumable that a similar mechanism takes place during periodontal wound healing and regeneration, including effects on the major components of the tooth-supporting apparatus (i.e., bone, cement, epithelium, and PDL).[31] Cell proliferation is also affected by the effect of both TNF-α[43] and *Pg* LPS.[44] A deficiency in cell density may influence periostin deposition into the ECM (Fig. 6). However, despite the effects of TNF-α and *Pg* LPS on cell proliferation, they also have an effect on periostin localization within the matrix (Fig. 6B); indirectly, by reducing periostin, an effect in cell proliferation and survival might be possible.

The present study shows less periostin (mRNA and protein) detection in a biomechanically challenged environment in conjunction with inflammatory mediators and bacterial virulence factors, and even more when combined, especially at 4 and 7 days. Furthermore, chronic exposure to inflammatory mediators and bacterial virulence factors are able to not only reduce periostin protein incorporation into the ECM but also availability in the environment (Fig. 3). It is important to consider that periostin levels in the cell lysates are affected by inflammatory mediators and bacterial virulence factors in both non-loaded and loaded conditions. However, the proportion of protein incorporated in the matrix was higher under mechanical stimulation (Fig. 2). Furthermore, differences in the supernatant among groups at longer time points (4 and 7 days) were significantly affected only under mechanical stimulation (Fig. 3B). However, an initial increase in periostin levels at 24 hours was observed.

Periostin is upregulated by TGF-β (Fig. 2). In previous studies,[5,6] it was demonstrated that mechanical stimulation increases TGF-β expression and, later, periostin expression. When blocking TGF-β with specific antibodies, periostin expression was decreased compared to non-blocked cultures.[5] However, as we show in the present study, cell culture supplementation with TGF-β in a non-loaded scenario does not have the same effects in terms of periostin incorporation within the cell matrix as the actual mechanical challenge. At this point, it cannot be concluded that either TGF-β increases levels of periostin to be secreted into the media or that loading condition prevents it. However, it is an interesting observation that a mechanical challenge, which increases periostin through a TGF-β signaling pathway, increases the proportion of periostin within the matrix versus the supernatant, whereas TGF-β supplementation does not have such a marked effect.

Conversely, as mentioned above, periostin is highly homologous to βIGH3.[10] They are expressed in the periodontium by PDL fibroblasts[8,21,45] and are

associated within the trans-Golgi network before secretion.[46] The protein structure of βIGH3 is identical to periostin but lacks the carboxyl-terminal region that is subject to alternative splicing in periostin.[10] In contrast, βIGH3 contains arginine-glycine-aspartic acid, in the one-letter amino acid code (RGD) sequence, which allows the heterodimer periostin–βIGH3 to interact with cell surface receptors. A possible contribution of βIGH3 has been suggested in the maintenance of the mechanical properties of the PDL by inhibiting mineralization[8] and osteogenesis.[47] Recent studies[48] using βIGH3, periostin, and periostin + βIGH3 KO mice have highlighted a cooperative action between secreted periostin and βIGH3. Periodontal breakdown was more severe in the periostin KO than in the βIGH3 KO and even worse in the double KO.[48] Therefore, βIGH3 fails to stabilize the effects of periostin loss, which supports the irreplaceable role of periostin in maintaining periodontal tissue integrity. According to our results, βIGH3 expression is also significantly influenced by chronic exposure to periodontal disease initiators (TNF-α and *Pg* LPS), although with a non-clear pattern among groups. The absence of both matricellular proteins by the effects of inflammatory cytokines and microbial virulence factors might then be markedly deleterious to the periodontium.

In the present study, in general, more marked deleterious effects were produced by the inflammatory component and the combination (Fig. 3). The specific mechanism of periostin expression reduction by bacterial byproducts and/or inflammatory mediators is still unknown. However, it is not the aim of this study to unravel such molecular events.

CONCLUSIONS

To the best of our knowledge, this is the first time that the ability of periodontal pathogen virulence factors and inflammatory mediators to reduce the expression and protein levels of periostin under in vitro biomechanical-simulated conditions has been evaluated. The feasibility of such a mechanism may contribute to identifying novel pathways in the periodontal disease pathogenesis and progression in vivo, because it would compromise the ability of the periodontium to maintain its integrity and can finally increase the severity and extent of the disease.

ACKNOWLEDGMENTS

This study was supported by National Institutes of Health/National Institute of Dental and Craniofacial Research Grants K23DE019872 (HFR) and F32DE021934 (JTM) and by Talentia Scholarship Program from the Regional Ministry for Innovation, Science, and Enterprise (Junta de Andalucía, Spain) (MP-M). The authors report no conflicts of interest related to this study.

REFERENCES

1. Takeshita S, Kikuno R, Tezuka K, Amann E. Osteoblast-specific factor 2: Cloning of a putative bone adhesion protein with homology with the insect protein fasciclin I. *Biochem J* 1993;294:271-278.
2. Fortunati D, Reppe S, Fjeldheim AK, Nielsen M, Gautvik VT, Gautvik KM. Periostin is a collagen associated bone matrix protein regulated by parathyroid hormone. *Matrix Biol* 2010;29:594-601.
3. Rios H, Koushik SV, Wang H, et al. Periostin null mice exhibit dwarfism, incisor enamel defects, and an early-onset periodontal disease-like phenotype. *Mol Cell Biol* 2005;25:11131-11144.
4. Kruzynska-Frejtag A, Wang J, Maeda M, et al. Periostin is expressed within the developing teeth at the sites of epithelial-mesenchymal interaction. *Dev Dyn* 2004; 229:857-868.
5. Rios HF, Ma D, Xie Y, et al. Periostin is essential for the integrity and function of the periodontal ligament during occlusal loading in mice. *J Periodontol* 2008; 79:1480-1490.
6. Horiuchi K, Amizuka N, Takeshita S, et al. Identification and characterization of a novel protein, periostin, with restricted expression to periosteum and periodontal ligament and increased expression by transforming growth factor beta. *J Bone Miner Res* 1999;14:1239-1249.
7. Afanador E, Yokozeki M, Oba Y, et al. Messenger RNA expression of periostin and Twist transiently decrease by occlusal hypofunction in mouse periodontal ligament. *Arch Oral Biol* 2005;50:1023-1031.
8. Ohno S, Doi T, Fujimoto K, et al. RGD-CAP (betaig-h3) exerts a negative regulatory function on mineralization in the human periodontal ligament. *J Dent Res* 2002; 81:822-825.
9. Hamilton DW. Functional role of periostin in development and wound repair: Implications for connective tissue disease. *J Cell Commun Signal* 2008;2:9-17.
10. Hoersch S, Andrade-Navarro MA. Periostin shows increased evolutionary plasticity in its alternatively spliced region. *BMC Evol Biol* 2010;10:30.
11. Page RC, Kornman KS. The pathogenesis of human periodontitis: An introduction. *Periodontol 2000* 1997; 14:9-11.
12. Ohshima M, Yamaguchi Y, Matsumoto N, et al. TGF-β signaling in gingival fibroblast-epithelial interaction. *J Dent Res* 2010;89:1315-1321.
13. Lin Z, Navarro VP, Kempeinen KM, et al. LMP1 regulates periodontal ligament progenitor cell proliferation and differentiation. *Bone* 2010;47:55-64.
14. Darveau RP, Hancock RE. Procedure for isolation of bacterial lipopolysaccharides from both smooth and rough *Pseudomonas aeruginosa* and *Salmonella typhimurium* strains. *J Bacteriol* 1983;155:831-838.
15. Loesche WJ, Bretz WA, Kerschensteiner D, et al. Development of a diagnostic test for anaerobic periodontal infections based on plaque hydrolysis of benzoyl-DL-arginine-naphthylamide. *J Clin Microbiol* 1990;28:1551-1559.
16. Pihlstrom BL, Michalowicz BS, Johnson NW. Periodontal diseases. *Lancet* 2005;366:1809-1820.
17. Socransky SS, Haffajee AD, Cugini MA, Smith C, Kent RL Jr. Microbial complexes in subgingival plaque. *J Clin Periodontol* 1998;25:134-144.

18. Reichenberger E, Baur S, Sukotjo C, Olsen BR, Karimbux NY, Nishimura I. Collagen XII mutation disrupts matrix structure of periodontal ligament and skin. *J Dent Res* 2000;79:1962-1968.
19. Sato R, Yamamoto H, Kasai K, Yamauchi M. Distribution pattern of versican, link protein and hyaluronic acid in the rat periodontal ligament during experimental tooth movement. *J Periodontal Res* 2002;37:15-22.
20. Long P, Liu F, Piesco NP, Kapur R, Agarwal S. Signaling by mechanical strain involves transcriptional regulation of proinflammatory genes in human periodontal ligament cells in vitro. *Bone* 2002;30:547-552.
21. Lindsley A, Li W, Wang J, Maeda N, Rogers R, Conway SJ. Comparison of the four mouse fasciclin-containing genes expression patterns during valvuloseptal morphogenesis. *Gene Expr Patterns* 2005;5:593-600.
22. Norris RA, Damon B, Mironov V, et al. Periostin regulates collagen fibrillogenesis and the biomechanical properties of connective tissues. *J Cell Biochem* 2007;101:695-711.
23. Norris RA, Kern CB, Wessels A, Wirrig EE, Markwald RR, Mjaatvedt CH. Detection of betaig-H3, a TGFbeta induced gene, during cardiac development and its complementary pattern with periostin. *Anat Embryol (Berl)* 2005;210:13-23.
24. Wilde J, Yokozeki M, Terai K, Kudo A, Moriyama K. The divergent expression of periostin mRNA in the periodontal ligament during experimental tooth movement. *Cell Tissue Res* 2003;312:345-351.
25. Oshima A, Tanabe H, Yan T, Lowe GN, Glackin CA, Kudo A. A novel mechanism for the regulation of osteoblast differentiation: Transcription of periostin, a member of the fasciclin I family, is regulated by the bHLH transcription factor, twist. *J Cell Biochem* 2002; 86:792-804.
26. Kii I, Amizuka N, Minqi L, Kitajima S, Saga Y, Kudo A. Periostin is an extracellular matrix protein required for eruption of incisors in mice. *Biochem Biophys Res Commun* 2006;342:766-772.
27. Kii I, Nishiyama T, Li M, et al. Incorporation of tenascin-C into the extracellular matrix by periostin underlies an extracellular meshwork architecture. *J Biol Chem* 2010;285:2028-2039.
28. Maruhashi T, Kii I, Saito M, Kudo A. Interaction between periostin and BMP-1 promotes proteolytic activation of lysyl oxidase. *J Biol Chem* 2010;285:13294-13303.
29. Saito Y, Yoshizawa T, Takizawa F, et al. A cell line with characteristics of the periodontal ligament fibroblasts is negatively regulated for mineralization and Runx2/Cbfa1/Osf2 activity, part of which can be overcome by bone morphogenetic protein-2. *J Cell Sci* 2002;115: 4191-4200.
30. Suzuki H, Amizuka N, Kii I, et al. Immunohistochemical localization of periostin in tooth and its surrounding tissues in mouse mandibles during development. *Anat Rec A Discov Mol Cell Evol Biol* 2004;281:1264-1275.
31. Park CH, Rios HF, Jin Q, et al. Tissue engineering bone-ligament complexes using fiber-guiding scaffolds. *Biomaterials* 2012;33:137-145.
32. Ma D, Zhang R, Sun Y, et al. A novel role of periostin in postnatal tooth formation and mineralization. *J Biol Chem* 2011;286:4302-4309.
33. Myokai F, Oyama M, Nishimura F, et al. Unique genes induced by mechanical stress in periodontal ligament cells. *J Periodontal Res* 2003;38:255-261.
34 Rios HF. The importance of periostin in the function of the periodontal ligament. [Thesis]. Kansas City, MO: University of Missouri–Kansas City; 2006. 127 p.
35. Yamaguchi M, Shimizu N, Goseki T, et al. Effect of different magnitudes of tension force on prostaglandin E2 production by human periodontal ligament cells. *Arch Oral Biol* 1994;39:877-884.
36. Yamaguchi M, Kasai K. Inflammation in periodontal tissues in response to mechanical forces. *Arch Immunol Ther Exp (Warsz)* 2005;53:388-398.
37. Ziegler N, Alonso A, Steinberg T, et al. Mechanotransduction in periodontal ligament cells identifies activated states of MAP-kinases p42/44 and p38-stress kinase as a mechanism for MMP-13 expression. *BMC Cell Biol* 2010;11:10.
38. Bao S, Ouyang G, Bai X, et al. Periostin potently promotes metastatic growth of colon cancer by augmenting cell survival via the Akt/PKB pathway. *Cancer Cell* 2004;5:329-339.
39. Kudo A. Periostin in fibrillogenesis for tissue regeneration: Periostin actions inside and outside the cell. *Cell Mol Life Sci* 2011;68:3201-3207.
40. Dorn GW 2nd. Periostin and myocardial repair, regeneration, and recovery. *N Engl J Med* 2007;357: 1552-1554.
41. Oka T, Xu J, Kaiser RA, et al. Genetic manipulation of periostin expression reveals a role in cardiac hypertrophy and ventricular remodeling. *Circ Res* 2007; 101:313-321.
42. Jackson-Boeters L, Wen W, Hamilton DW. Periostin localizes to cells in normal skin, but is associated with the extracellular matrix during wound repair. *J Cell Commun Signal* 2009;3:125-133.
43. Gaur U, Aggarwal BB. Regulation of proliferation, survival and apoptosis by members of the TNF superfamily. *Biochem Pharmacol* 2003;66:1403-1408.
44. Takemura A, Matsuda N, Kimura S, Fujiwara T, Nakagawa I, Hamada S. *Porphyromonas gingivalis* lipopolysaccharide modulates the responsiveness of human periodontal ligament fibroblasts to platelet-derived growth factor. *J Periodontal Res* 1998;33:400-407.
45. Doi T, Ohno S, Tanimoto K, et al. Mechanical stimuli enhances the expression of RGD-CAP/betaig-h3 in the periodontal ligament. *Arch Oral Biol* 2003;48: 573-579.
46. Kim BY, Olzmann JA, Choi SI, et al. Corneal dystrophy-associated R124H mutation disrupts TGFBI interaction with Periostin and causes mislocalization to the lysosome. *J Biol Chem* 2009;284:19580-19591.
47. Kim JE, Kim EH, Han EH, et al. A TGF-beta-inducible cell adhesion molecule, betaig-h3, is downregulated in melorheostosis and involved in osteogenesis. *J Cell Biochem* 2000;77:169-178.
48. RiosH, Tomanicek-Volk S, Benavides E, Conway SJ. βig-H3 fails to compensate for periostin absence in the periodontium. *J Dent Res 89 (Spec Iss B)* 2010. Available at www.dentalresearch.org. Accessed January 31, 2012.

Correspondence: Dr. Hector F. Rios, 1011 N. University Ave., Office 3349, Ann Arbor, MI 48109-1078. Fax: 734/763-5503; e-mail: hrios@umich.edu.

Submitted January 31, 2012; accepted for publication June 4, 2012.